DOI: 10.15825/1995-1191-2022-3-80-93

RESULTS OF PRECLINICAL TRIALS IN A SHEEP MODEL OF BIODEGRADABLE SMALL-DIAMETER VASCULAR GRAFTS

L.V. Antonova, E.O. Krivkina, M.Yu. Khanova, E.A. Velikanova, V.G. Matveeva, A.V. Mironov, A.R. Shabaev, E.A. Senokosova, T.V. Glushkova, M.Yu. Sinitsky, R.A. Mukhamadiyarov, L.S. Barbarash

Research Institute for Complex Issues of Cardiovascular Diseases, Kemerovo, Russian Federation

Surface modification of polymer vascular matrices is a promising development for preventing vascular graft thrombosis, improving long-term patency and accelerating remodeling. **Objective:** to study the outcomes of long-term patency of PHBV/PCL/GFmix grafts with iloprost (Ilo) and heparin (Hep) implanted into the carotid artery of sheep. **Materials and methods.** Matrices ∅4 mm were fabricated by electrospinning from a polymer composition of poly(3-hydroxybutyrate-co-3-hydroxyvalerate) (PHBV) and poly(ε-caprolactone) (PCL) with incorporation of endothelial growth factor (VEGF), basic fibroblast growth factor (bFGF) and chemoattractant molecule (SDF-1α). The fabricated matrices were then modified with Ilo and Hep by complexation via polyvinylpyrrolidone (PVP). Synthetic Gore-Tex grafts were used as a comparison group. The physical and mechanical properties of the studied matrix groups were evaluated, the surface structure of vascular grafts before and after implantation was assessed. Vascular grafts were implanted into the carotid artery of a sheep. The explanted samples were studied via histological and immunofluorescence analysis, the elemental composition of the obtained vascular graft samples was also assessed, and the gene expression profile was evaluated. **Results.** One day after implantation, the patency of PHBV/PCL/GFmix$^{Hep/Ilo}$ vascular grafts was 62.5%, whereas synthetic Gore-Tex grafts had thrombosis in 100% of cases. At the same time, after 18 months of implantation, the patency of biodegradable PHBV/PCL/GFmix$^{Hep/Ilo}$ vascular grafts decreased to 50%. Permeable drug-coated polymer grafts were completely reabsorbed after 18 months of implantation, and aneurysmally dilated newly-formed vascular tissue was formed in their place. **Conclusion**. Modification of the surface of PHBV/PCL/GFmix polymer grafts with Hep + Ilo coating improved long-term patency outcomes compared to synthetic Gore-Tex grafts.

Keywords: vascular grafts, anti-thrombogenic coating, electrospinning, implantation, heparin, iloprost.

INTRODUCTION

At present, there has been a continuous increase in the incidence of atherosclerosis among the population, including coronary artery lesions and peripheral artery disease [1–5].

Therefore, there is an increasing number of surgical interventions using prosthetic implants, shunts and patches to restore effective blood flow in damaged blood vessels [6]. The best option for surgical treatment of the above pathology is the use of autologous material (own blood vessels), which is currently the gold standard. However, these grafts have limited availability due to previous operations with these vessels, progressive atherosclerosis and other diseases [7]. In addition, the graft harvesting process and subsequent evaluation before implantation can damage the vessel and lead to endothelial dysfunction, proinflammatory response and, ultimately, graft thrombosis and occlusion. High failure rates make this treatment option largely inadequate, leading to the development of non-autologous alternatives [8–10]. Xenogeneic and synthetic products currently used in clinical practice are well suited for large-diameter vascular grafts but are at high risk of thrombosis. For small-diameter vascular grafts, there is the risk of neointimal hyperplasia in the late postoperative period [7, 11–13].

In this regard, the lack of cardiovascular surgery products that are based on alternative materials and do not cause such complications is the most pressing problem. One of the promising modern fields involved in the development of vascular grafts is vascular tissue engineering [14–17], which allows using non-standard types of materials (biodegradable polymers, natural polymers, autologous biological fluids and tissues) for creating medical devices, as well as original approaches to their manufacturing, ensuring porosity of created structures and, consequently, effective migration of own cells into the wall of these structures to form in situ new healthy tissue [18–22].

However, due to high porosity and prolonged resorption involving monocyte-macrophage system cells, nonwoven biodegradable matrices can also provoke thrombus formation [23–26]. Additional modification

Corresponding author: Evgeniya Krivkina. Address: 6, Sosnovy Boulevard, Kemerovo, 650002, Russian Federation. Phone: (908) 946-66-39. E-mail: leonora92@mail.ru

of the surface of tissue-engineered highly porous vascular grafts with antiplatelet and anticoagulant drugs, which can prevent thrombotic processes after implantation of such grafts into the vascular bed, can be a solution. Additional introduction of bioactive substances such as growth factors, chemokines, interleukins, amino acids and others into the prosthesis structure and their prolonged release can imitate natural biochemical signals and guide the regeneration process with the formation of all structural layers of vascular tissue, including endothelium [27–29].

Thus, highly porous biodegradable constructs need additional modification of their surface with anti-thrombogenic substances in order to avoid the risk of failure after implantation of such a construct in the vascular bed [30, 31].

MATERIALS AND METHODS

Fabrication of vascular grafts

PHBV/PCL vascular grafts ∅4 mm in diameter and 40.0 mm long were fabricated by two-phase electrospinning from 5% PHBV (Sigma-Aldrich, USA) and 10% PCL (Sigma-Aldrich, USA) on a Nanon-01A apparatus (MECC, Japan). Chemically pure chloroform (Vekton, Russia) was used as a solvent.

To incorporate the growth factor and chemoattractant molecules into the polymer fiber, a PHBV/PCL chloroform solution was thoroughly mixed with a 20:1 solution of one or more differentiation factors diluted in phosphate-buffered saline (PBS; Gibco, USA) to form a suspension. One-third of the inner part of the prosthetic wall was made from PHBV/PCL solution, with the addition of human vascular endothelial growth factor (VEGF; Sigma-Aldrich, USA). The outer two-third part of the prosthetic wall was made from PHBV/PCL solution with a mixture of recombinant human basic fibroblast growth factor (bFGF; Sigma-Aldrich, USA) and recombinant human chemoattractant molecule, stromal cell-derived factor-1α (SDF-1α; Sigma-Aldrich, USA).

Formation of an anti-thrombogenic coating on the surface of biodegradable vascular grafts

The surface of the PHBV/PCL/GFmix graft was additionally modified with antiplatelet agents and anticoagulants according to our own original method to increase thromboresistance [32].

To modify the internal surface of the graft, 10.0% solution of PVP (PanReac, Germany) was prepared in ethanol. The prosthesis was immersed in the PVP solution for 30 minutes, filling its internal canal completely with the solution. The prosthesis was then removed from the solution and dried horizontally for 24 hours.

To graft PVP to the surface of the polymer prosthesis, the product was placed in a glass tube that was filled with inert argon gas and irradiated with ionizing radiation with 15 kGy total absorbed dose.

Before drug adhesion, non-grafted PVP residues were three times washed off the surface of the vascular graft placed in tubes with sterile water for injection. Each wash lasted for 30 minutes.

A modifying solution consisting of glycine buffer solution (pH = 2.5–2.6) with the anticoagulant Hep (Diamed-Pharma, Russia) at 5000 IU/ml concentration and antiplatelet agent Ilo (Bayer, Germany) at 0.2 μg/ml concentration was prepared in sterile conditions. To attach the drugs to the remaining free reactive groups of the grafted PVP, the vascular grafts were incubated in the modifying solution for 30 minutes. Then, they were air-dried under sterile conditions for 24 hours.

Assessment of physical and mechanical properties

The mechanical properties of PHBV/PCL biodegradable drug-coated vascular grafts before and after formation of an additional anti-thrombogenic drug coating were evaluated under uniaxial tension conditions on a Z-series universal testing machine (Zwick/Roell). The ultimate tensile strength of the material was estimated as the maximum tensile stress (MPa) before failure. The stress-strain properties of the material were evaluated by relative elongation to failure (%) and Young's modulus (MPa). Synthetic Gore-Tex graft (ST04010A, USA), native human internal thoracic artery (a. mammaria), and sheep carotid artery were used as controls.

Scanning electron microscopy

The surface structure of biodegradable PHBV/PCL/GFmix vascular grafts before and after formation of anti-thrombogenic drug coating, as well as synthetic Gore-Tex vascular grafts was assessed on scanning electron microscope S-3400N (Hitachi, Japan) under high vacuum at 10 kV accelerating voltage. Before the study, 0.5 × 0.5 cm prosthesis samples were subjected to gold-palladium sputtering to obtain a 15 nm thick coating using sputtering system EM ACE200 (Leica Mikrosysteme GmbH, Austria).

Implantation of vascular grafts into the carotid artery of sheep

All groups of vascular grafts were implanted into the carotid artery of Edilbay sheep. The experimental group of PHBV/PCL/GFmix$^{Hep/Ilo}$ prostheses (n = 8) was implanted for 18 months.

Synthetic Gore-Tex® grafts (Number ST04010A, USA), (n = 5) implanted in the carotid artery of sheep for 6 months (taking into account their early thrombosis 1 day after implantation) were used as the comparison group.

Anaesthetic support

Premedication: xylazine (Xylanit) 0.05–0.25 ml per 10 kg of animal weight + atropine 1 mg intramuscularly. Anesthesia induction: 5–7 mg of propofol per 1 kg of animal weight, within 90 seconds after – atracurium besylate (Ridelat) was administered intravenously in a 0.5–0.6 mg/kg dose. Tracheal intubation with a 9.0 diameter endotracheal tube. Anesthesia maintenance: Sevoran 2–4 vol%, continuous infusion of Ridelat at 03–0.6 mg/kg/h.

Main stage of vascular graft implantation

Access to the carotid artery; systemic heparinization – 5000 units administered intravenously; carotid artery clamping, resection of the isolated segment at a 45-degree angle, end-to-end implantation of vascular grafts with continuous twist suture proximally and then distally with prolene 6/0 sutures (Ethicon, USA). Standard protocol for prevention of air embolism and triggering of blood flow; wound closure with Vicril 2.0 suture (Ethicon, USA); suture treatment with butyral phenolic adhesive, sodium enoxaparin subcutaneously 4,000 IU anti-Xa/0.4 ml; extubation.

Intraoperative drug administration: infusion of 0.9% NaCl 500 mL – IV drip; Axetine (cefuroxime) 1.5 g – IV drip; Postoperative drug therapy: antibiotic therapy (Axetine (cefuroxime) 1.5 g – intramuscular twice/day + Enoxaparin sodium subcutaneously 4,000 IU anti-Xa/0.4 ml for 5 days. With proven patency of biodegradable prostheses: clopidogrel 75 mg orally once/day + sodium heparin 5000 units subcutaneously twice/day) – for 1 month.

Postoperative ultrasound screening of patency in implanted vascular grafts: for permeable prostheses – day 1 and 5, then once every 3 months up to the estimated date of animal's withdrawal from the experiment; for thrombosed grafts – day 1 and 5.

Histopathology

Explanted prosthetic specimens were subjected to histological examination with H&E stain, Van Gieson's stain, orcein stain, and alizarin red S stain.

The explanted specimens were fixed in formalin for 24 hours, then washed with running tap water to remove the fixative solution, and dehydrated in IsoPrep (BioVitrum, Russia). Samples were impregnated with paraffin (3 portions) at 56 °C for 60 minutes in each portion. Impregnated samples were filled with Histomix paraffin (BioVitrum, Russia). From the obtained samples, 8 μm thick sections were made using an HM 325 rotary microtome (Thermo Scientific, USA). The samples were then placed in an oven and dried overnight at 37 °C. After complete drying, samples were deparaffinized in o-xylene (3 portions) for 1–2 minutes and dehydrated in 96% alcohol (3 portions) for 1–2 minutes. The deparaffinized sections were then stained according to the staining protocol. The samples were examined by light and fluorescence microscopy using an AXIO Imager A1 microscope (Carl Zeiss, Germany) with 50×, 100×, and 200× magnifications.

Confocal fluorescence microscopy

From frozen explanted specimens, 8-μm-thick sections were made using a cryotome (Microm HM 525, Thermo Scientific).

The sections were fixed in 4% paraformaldehyde solution for 10 minutes.

Before staining for intracellular markers, the sections were permeabilized with Triton-X100 solution (Sigma-Aldrich, USA) for 15 minutes. The prepared sections were stained using specific primary antibodies: rabbit anti-CD31 antibodies (Abcam, UK) and mouse alpha smooth muscle actin antibodies (α-SMA, Abcam, UK); rabbit antibodies to von Willebrand factor (vWF, Abcam, UK); rabbit antibodies to collagen type IV (Abcam, UK) and mouse collagen type I antibodies (Abcam, UK); rabbit collagen type III antibodies (Novus Biologicals, USA). The sections were incubated with primary antibodies overnight at 4 °C, then with secondary donkey anti-mouse IgG antibody conjugated with Alexa Fluor 488-conjugated (Thermo Fisher, USA) and donkey anti-mouse IgG antibody conjugated with Alexa Fluor 555-conjugated (Thermo Fisher Scientific, USA) for 1 hour at room temperature. At all staining stages, phosphate-buffered saline with 0.1% Tween (Sigma-Aldrich, USA) was used for intermediate washing of the sections. To remove autofluorescence, the sections were treated with Autofluorescence Eliminator Reagent (Millipore, USA) according to the manufacturer's procedure. Nuclei were contrasted using DAPI stain (10 μg/mL, Sigma-Aldrich, USA) for 30 minutes. The preparations were analyzed using a confocal laser scanning microscope LSM 700 (Carl Zeiss, Germany).

Examination of explanted vascular graft samples by SEM according to the original technique

The explanted samples were fixed in formalin for 24 hours, then postfixed with 1% osmium tetroxide in 0.1 M phosphate buffer and stained with 2% osmium tetroxide in double distilled water for 48 hours. The samples were then dehydrated in a series of alcohols of increasing concentration, stained with 2% uranyl acetate (Electron Microscopy Sciences, USA) in 95% ethanol, dehydrated with 99.7% isopropanol (BioVitrum, Russia) for 5 hours and with acetone (Reachim, Russia) for 1 hour, impregnated with a mixture of acetone and Epon epoxy resin (Electron Microscopy Sciences, USA) in a 1:1 ratio (6 hours), then transferred to a fresh portion of epoxy resin (for 24 hours) and further polymerized

in FixiForm containers (Electron Microscopy Sciences, USA) at 60 °C. After that, the samples in epoxy blocks were grinded and polished on a TegraPol-11 machine (Struers, USA). Lead citrate contrasting was performed by Reynolds's stain for 7 minutes by applying the solution to the surface of the ground sample followed by washing with double distilled water. Next, epoxy carbon blocks (10–15 nm coating thickness) were sprayed on the polished surface using a vacuum sputtering station (EM ACE200, Leica). The structure of the samples was visualized by scanning electron microscopy in backscattered electrons using a Hitachi-S-3400N electron microscope (Hitachi, Japan) in the BSECOMP mode at 10 kV accelerating voltage.

Examination of the elemental composition of explanted vascular graft samples

To assess the elemental composition of the examined samples, we used X-ray spectral microanalysis performed using XFlash 4010 energy dispersive spectrometer (Bruker), which is a part of S-3400N scanning electron microscope (Hitachi). Elemental analysis was carried out under conditions of low vacuum (20 Pa pressure in the microscope chamber) and at 15 kV accelerating voltage in a scanning electron microscopy mode in backscattered electrons, without using standard samples. Macrophages, giant multinucleated cells, neutrophils, smooth muscle and mast cells were identified on digital photomicrographs, their localization and interaction between themselves and with other vascular graft elements were determined.

Comparative assessment of gene expression profile characteristic of native vascular tissue in the wall of the explanted vascular graft and native sheep carotid artery

To assess gene expression, the materials used were dissected sections of the vascular graft and carotid artery, as well as endothelial cell wash obtained by washing the vessels and prosthesis with lysis reagent TRIzol (Invitrogen, USA). The genes of interest were *IL1B, IL6, IL6, IL10, IL8, IL12A, TNF, VEGF, CXCR4, NR2F2, SNAI2, ICAM1, YAP1, IFNG, KDR, FGF2, MMP2*, and *TGFB*. Immediately after resection, a section of the vascular graft or carotid artery was placed in a test tube containing 900 μL of TRIzol (Invitrogen, USA) for further RNA isolation. Before starting the experiment, all work surfaces and laboratory equipment were treated with decontamination solution RNaseZapTM RNase (Invitrogen, USA). Samples were homogenized on an apparatus (MP Biomedicals, USA). RNA was isolated according to the standard protocol using the Chomczynski method (guanidinium thiocyanate-phenol-chloroform extraction). The amount and quality of isolated RNA were assessed using a NanoDropTM 2000 spectrophotometer (ThermoScientific, USA). RNA integrity was determined using a Qubit 4 Fluorometer spectrophotometer (Invitrogen, USA) by measuring the RIQ (RNA Integrity and Quality) index. A complementary DNA (cDNA) molecule was synthesized from 100 ng of isolated RNA using reverse transcription reaction and a commercial High-Capacity cDNA Reverse Transcription Kit (Applied Biosystems, USA). The quantity and quality of the synthesized cDNA were assessed using a NanoDropTM 2000 spectrophotometer (ThermoScientific, USA). Gene expression was assessed by quantitative polymerase chain reaction (qPCR) with real-time detection of amplification products with SYBR fluorescent dye on a ViiA 7 Real-Time PCR System amplifier (Applied Biosystems, USA). For each sample, 10 μl of reaction mixture was prepared, containing 5 μl of PowerUpTM SYBR® Green Master Mix (Applied Biosystems, USA), a mixture of forward and reverse primers at 500 nM final concentration, and 10 ng of cDNA. PCR was performed in a 96-well optical plate containing, in addition to the samples analyzed, five standards with double dilution and a negative control (reaction mixture without cDNA). Three technical replicates were prepared for each analyte, standard, and negative control. Amplification was performed according to the following scheme: 2 minutes at 50 °C, 2 minutes at 95 °C, 15 seconds at 95 °C, and 1 minute at 60 °C (40 cycles). Reaction specificity and efficiency were checked by analyzing melting curves and amplification plots in QuantStudioTM Real-Time PCR Software v.1.3 (Applied Biosystems, USA). PCR results were normalized using three reference genes ACTB, GAPDH, and B2M in accordance with available recommendations. Expression of the studied genes was calculated by the $2^{-\Delta\Delta\Delta C}{}_{T}$ method and expressed as a multiple change relative to control samples.

Statistical analysis

Study results were processed using GraphPad Prism (Graph Pad Software). Normality of distribution was assessed using the Kolmogorov–Smirnov test. Significance of differences between two independent groups was determined using nonparametric Mann–Whitney test. Nonparametric Kruskel–Wallis analysis of variance was used to compare three or more independent groups; Dunn's test was used for pairwise comparison of groups. Differences were considered statistically significant at $p < 0.05$. Data are presented as mean and standard deviation M ± SD, as well as median and 25th and 75th percentiles Me (25%; 75%).

RESULTS

Study of mechanical properties

The study of physical and mechanical properties revealed a statistically significant increase in the stiffness of PHBV/PCL/GFmix vascular grafts after modification with PVP and subsequent complexation with Hep and

Ilo (Table). The Young's modulus values of PHBV/PCL/GFmix$^{Hep/Ilo}$ grafts were 5.8 times higher than that of PHBV/PCL/GFmix and 20.6 times higher than that of a. mammaria ($p < 0.05$), and that of sheep carotid artery was 100 times higher. Also, biodegradable PHBV/PCL/GFmix$^{Hep/Ilo}$ drug-coated vascular grafts had the maximum force applied to the specimen before its destruction (Table). The relative elongation of PHBV/PCL/GFmix and PHBV/PCL/GFmix$^{Hep/Ilo}$ vascular grafts exceeded that of a. mammaria almost 4-fold ($p < 0.05$); for carotid artery, there was a 0.3-fold decrease. There were no significant differences between a. mammaria and polymer vascular grafts in terms of tension. Gore-Tex® synthetic grafts had good elastic properties similar to those of the native vessel, but at the same time had great strength. Therefore, the force applied to Gore-Tex® grafts before their destruction was more than 6 times greater than that of biodegradable prostheses and 22.9 times greater than that of a. mammaria ($p < 0.05$). The increased stiffness of the PHBV/PCL/GFmix$^{Hep/Ilo}$ drug-coated vascular grafts is probably due to graft surface polymerization with PVP and exposure to ionizing radiation.

Scanning electron microscopy of vascular grafts before and after surface modification with drugs

The surface of PHBV/PCL/GFmix grafts was modified with antithrombotic drugs by forming a PVP hydrogel coating on its inner surface, which is able not only to bind drugs as a result of complexation, but also temporarily (until its complete resorption) occupy the pore cavity, thereby reducing the risk of platelet adhesion to the prosthesis surface after implantation in the vascular bed. Besides, PVP's well-known hydrophilicity helps to reduce the degree of adhesion of protein molecules and blood cells, in particular, platelets, as well as prevent conformational changes in protein structures. Mobility of macromolecular chains in hydrogels, among other things, is due to the high desorption rate of protein molecules, which complements the spectrum of reasons for their anti-thrombogenic potential [33, 34]. The PHBV/PCL/GFmix$^{Hep/Ilo}$ grafts consisted of chaotically arranged microsized polymer fibers, 1.47 ± 0.67 μm in diameter (Fig. 1), forming micropores during their interlacing. Fig. 1 shows that after washing off the residual unpolymerized PVP from the graft surface and subsequent Hep and Ilo attachment to the remaining free reactive groups of PVP, the initial architectonics of the polymer matrix surface was preserved, and the water-soluble polymer covered only the surface of threads forming the tubular framework, without changing the appearance of micropores. The formed drug coating was sufficient to significantly improve the hemocompatibility properties of the graft surface, which had been previously proven in in vitro experiments: the maximum platelet aggregation after contact with graft surface with drug-coated PHBV/PCL/GFmix$^{Hep/Ilo}$ decreased by 2.1 times compared to analogous prostheses without drug-coated PHBV/PCL/GFmix. Against this background, platelet deformation index after contact with the surfaces of PHBV/PCL/GFmix$^{Hep/Ilo}$ and PHBV/PCL/GFmix grafts was 0 and 2.7, respectively [35].

The inner surface of Gore-Tex® synthetic grafts is represented by monolithic polymer fragments (Fig. 1), alternating with porous structures. The pores on the inner surface of Gore-Tex® are larger than those on the surface of PHBV/PCL/GFmix$^{Hep/Ilo}$.

Vascular graft implantation outcomes

A sheep model was used for preclinical testing of the developed grafts. It is the model of choice for in vivo evaluation of the effectiveness of cardiovascular implants [36]. It is believed that sheep are suitable for "worst-case modeling" due to the increased propensity of their vessels to thrombosis and calcification, which

Table

Mechanical properties of PHBV/PCL/GFmix polymer grafts before and after formation of antithrombogenic drug coating in comparison with Gore-Tex®, a. mammaria and sheep carotid artery

	Tension, MPa	Relative elongation, %	Young's modulus (E_{mod}), MPa
PHBV/PCL/GFmix (n = 9) M (25–75%)	3.045 (2.9; 3.2)$^{\&}$	121.7 (117.1; 129.6)$^{\#\,\&}$	8.6 (8.0; 9.64)$^{\#\,\&}$
PHBV/PCL/GFmix$^{Hep/Ilo}$ (n = 9) M (25–75%)	3.94 (3.78–3.99)$^{\&}$	109.17 (92.29–116.06)$^{\#\,\&}$	49.95 (44.9–54.7)*$^{\#\,\&}$
Gore-Tex® (n = 9) M (25–75%)	22.95 (22.42–23.47)**	337.0 (332.0–341.8)**	1.98 (1.36–2.59)
A. mammaria (n = 9) M (25–75%)	2.48 (1.36–3.25)$^{\&}$	29.72 (23.51–39.62)$^{\&}$	2.42 (1.87–3.19)
Sheep carotid artery	1.2 (1.06–1.9)	158.5 (126.0–169.5)	0.49 (0.39–0.66)

Note: *, $p < 0.05$ relative to PHBV/PCL/GFmix; $^{\#}$, $p < 0.05$ relative to a. mammaria; **, relative to all groups considered; $^{\&}$, relative to Gore-Tex®.

allows for the most rigorous testing of vascular grafts for their long-term patency and degeneration in vivo [36].

The need to form an anti-thrombogenic drug coating was down to the negative outcomes obtained earlier in the implantation of biodegradable PHBV/PCL/GFmix vascular prostheses into a sheep carotid artery [37]. High porosity of the wall resulted in early graft thrombosis in 100% of cases [37].

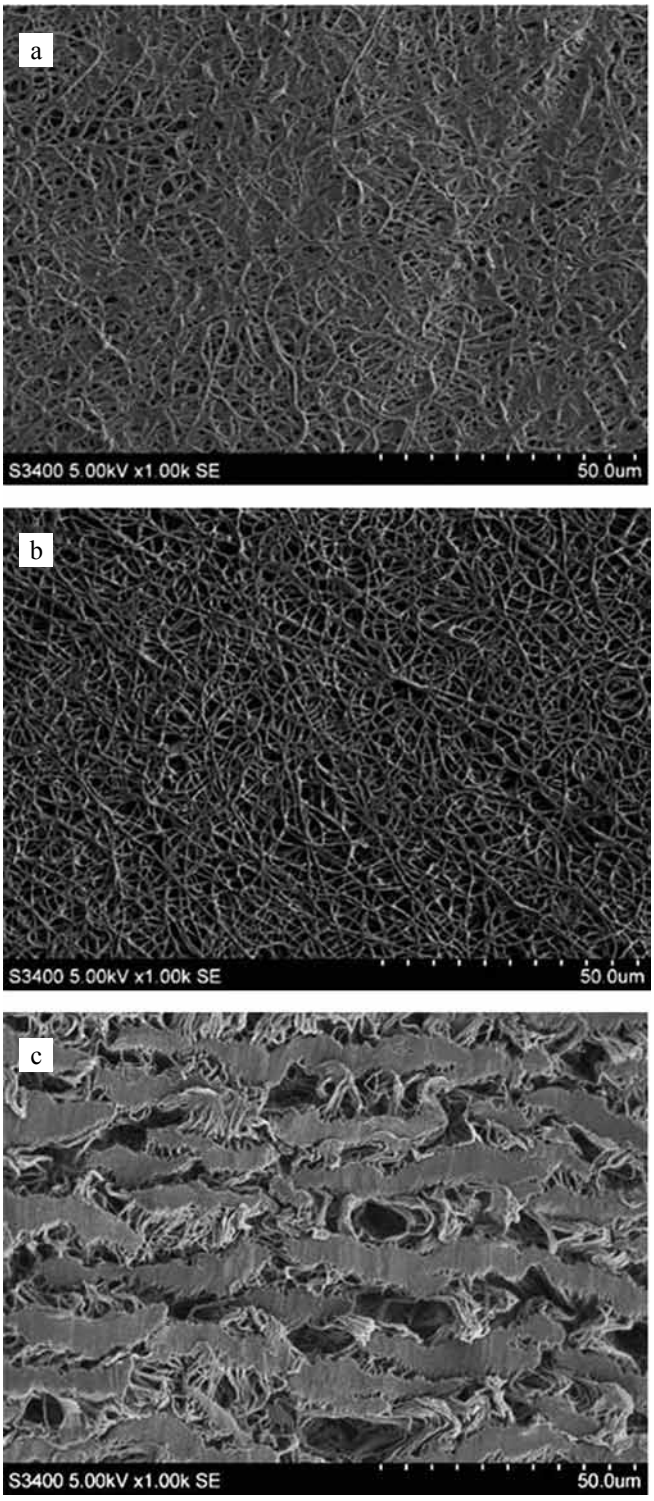

Fig. 1. Scanning electron microscopy of the inner surface of biodegradable and synthetic vascular grafts: a, inner surface of PHBV/PCL/GFmix$^{Hep/Ilo}$ graft before washing against PVP; b, inner surface of PHBV/PCL/GFmix$^{Hep/Ilo}$ graft after washing against PVP; c, inner surface of Gore-Tex® graft. 1000× magnification

In order to compare the effectiveness of the developed drug-coated vascular grafts with the grafts currently used in clinical practice, a comparison group of 4 mm-diameter synthetic Gore-Tex® grafts (Number ST04010A, USA) was also formed.

Patency of the PHBV/PCL/GFmix$^{Hep/Ilo}$ drug-coated grafts was 62.5% (5 of 8) 1 day after implantation in a sheep carotid artery (Fig. 2). After 18 months, patency of the PHBV/PCL/GFmix$^{Hep/Ilo}$ graft was 50.0%. However, all explanted prostheses that were permeable exhibited aneurysmal wall dilation throughout (Fig. 2).

One day after implantation of Gore-Tex® grafts, thrombosis was detected in 100.0% of cases (5 out of 5) (Fig. 2).

Outcomes of morphological study of explanted grafts

It was revealed that in place of the biodegradable vascular graft PHBV/PCL/GFmix$^{Hep/Ilo}$, a three-layer newly formed vessel similar in structure to native carotid artery was formed. However, the main difference between the newly formed vascular tissue and the native vessel tissue was aneurysmal dilation, absence of elastic fibers and clear elongation of smooth muscle cell cytoplasm, which is probably due to aneurysmal stretching of the formed vascular tissue under pulsatile blood flow conditions (Fig. 3). A small focus of coarse-grained calcium was detected in the thickness of only one PHBV/PCL/GFmix$^{Hep/Ilo}$ graft – between the media and adventitia (Fig. 3).

Recanalized thrombus was detected in the lumen of all explanted Gore-Tex® grafts 6 months after implantation. A thick connective tissue capsule was formed on the outside around the prosthesis. There was no formation of newly formed tissue in the graft thickness (Fig. 3). Despite the absence of blood flow, the Gore-Tex® graft underwent massive calcification (Fig. 3). Fine-grained calcium foci were also found in the outer connective tissue capsule. Nothing similar was found in the thrombosed PHBV/PCL/GFmix grafts implanted earlier in a sheep carotid artery for 12 months [37].

Examination of the explanted biodegradable PHBV/PCL/GFmixHep/Ilo drug-coated grafts by SEM revealed endothelial cells typical in morphology (Fig. 3). Examination of the thickness of the explanted prostheses showed that the newly formed vascular tissue that formed in place of the reabsorbed biodegradable tubular skeleton had three layers: neointima consisting of smooth muscle cells and covered by endothelium; the middle layer containing a large number of collagen fibers, fibroblast-like cells, macrophages, single giant multinucleated cells and vasa vasorum (Fig. 3). A small area of calcium deposition

was found at the junction between the neointima and the middle layer (Fig. 3). The middle layer was followed by the outer layer containing all elements typical for adventitia: vasa vasorum, single cells of a foreign body, perivascular fatty tissue, lymphoid follicles (Fig. 3).

A detailed layer-by-layer SEM study of the tissues formed around the explanted Gore-Tex® graft revealed that the entire lumen was filled with recanalized thrombus (Fig. 3). The prosthesis wall contained calcium inclusions, occupying 12–15% of the area (Fig. 3). Outside, the graft was surrounded by a layer of dense connective tissue consisting predominantly of fibrocytes and collagen fibers with a large number of newly formed vessels (Fig. 3). Calcium deposits were represented by shapeless heterogeneous formations often without clearly defined boundaries (Fig. 3). The internal structure of the calcifications was heterogeneous. In the deposit areas with minimal amounts of calcium, its presence was noted only in the outer part of the fibers forming the prosthesis (Fig. 3). With more pronounced calcification, calcium deposits were observed both in the outer structure of the fibers and in the space between them (Fig. 3). In the variant with maximum calcification, practically the entire space was filled with calcium deposits, inside which there were individual non-calcified fibers (Fig. 3).

Outcomes of confocal fluorescence microscopy

Immunofluorescence study of the explanted drug-coated grafts showed that the tissue formed in the place of the reabsorbed graft contained the main structural elements of the newly formed vessel: endothelial and smooth muscle layers were formed, a great number of collagens type I, III and IV was revealed. Collagen type IV was predominantly deposited in basal membrane, collagen type III – in basal membrane and graft wall, collagen type I – in adventitia (Fig. 4). The endothelial layer lining the neointima was represented by a double-row arrangement of endothelial cells active in terms of vWF synthesis, but simultaneously expressing CD31 and α-actin (Fig. 4). Such a picture may indirectly indicate the presence of endothelial-to-mesenchymal transition (EndMT), which can be triggered under conditions that are not physiological for the endothelium. In an aneurysmally dilated implant, turbulent blood flow may well be the cause capable of triggering the EndMT. Clusters of CD31 and vWF-positive endothelial cells were noted in the thickness of the prosthetic wall. Dense ordered tissue formed by actin-secreting cells with concentrically oriented clusters of vWF-secreting cells and collagen type III strands were found along the outer edge and outside of PHBV/PCL/GFmix$^{Hep/Ilo}$ graft (Fig. 4). It was revealed that the cells lining the neointimal surface

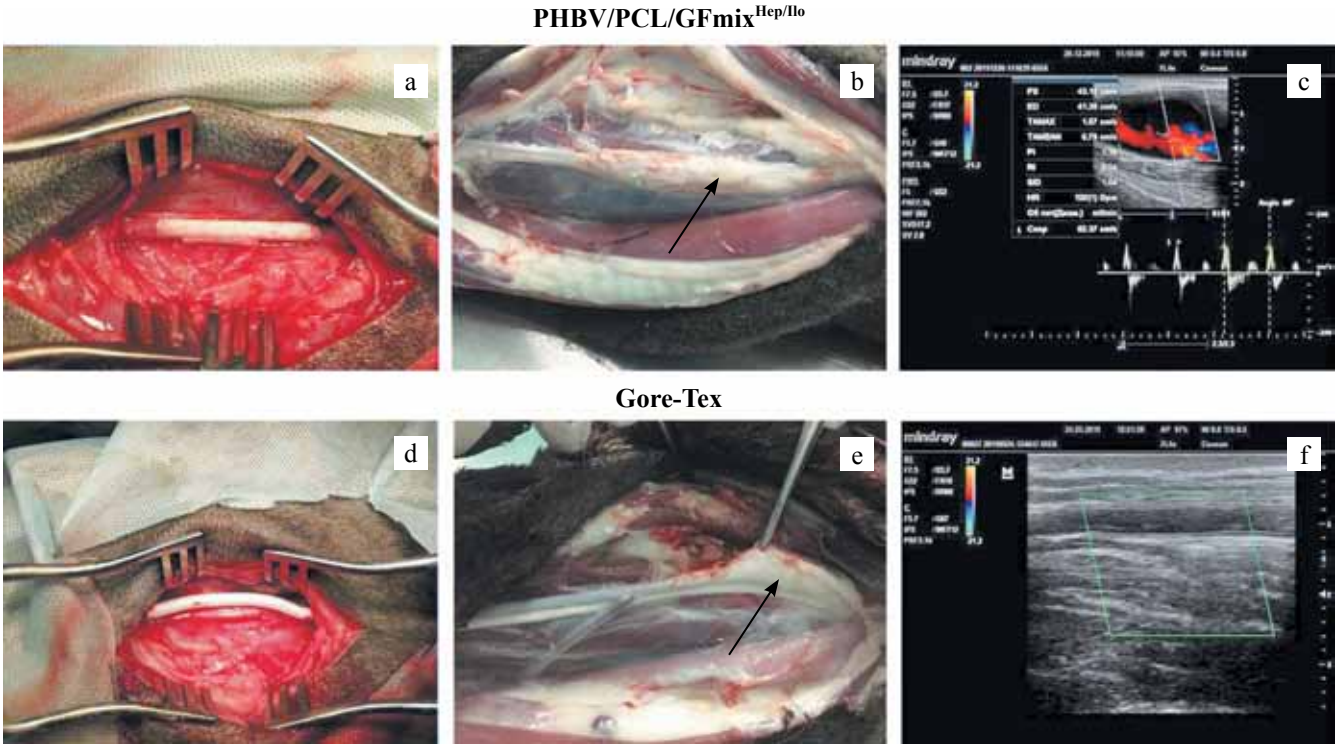

Fig. 2. Appearance and permeability analysis of PHBV/PCL/GFmix$^{Hep/Ilo}$ and Gore-Tex grafts: a, PHBV/PCL/GFmix$^{Hep/Ilo}$ implanted in the sheep carotid artery; b, PHBV/PCL/GFmix$^{Hep/Ilo}$ 18 months after implantation; c, ultrasound image of patency of PHBV/PCL/GFmix$^{Hep/Ilo}$ graft 18 months after implantation; d, Gore-Tex implanted in sheep carotid artery; e, Gore-Tex after 6 months of implantation; f, ultrasound image of Gore-Tex patency

in a monolayer from the vessel lumen side were mature endothelial cells synthesizing vWF, but with signs of EndMT (simultaneously expressing CD31 and α-actin). There was a basal membrane with collagen type IV. Collagen type III was found in the wall and in the basal membrane under the endothelial cell layer (Fig. 4). In the thickness of the explant wall and adventitial layer there was a large number of newly formed vessels and cellular elements (Fig. 4).

Immunofluorescence examination of synthetic Gore-Tex® vascular grafts after 6 months of implantation revealed an obstructive thrombus in the graft lumen;

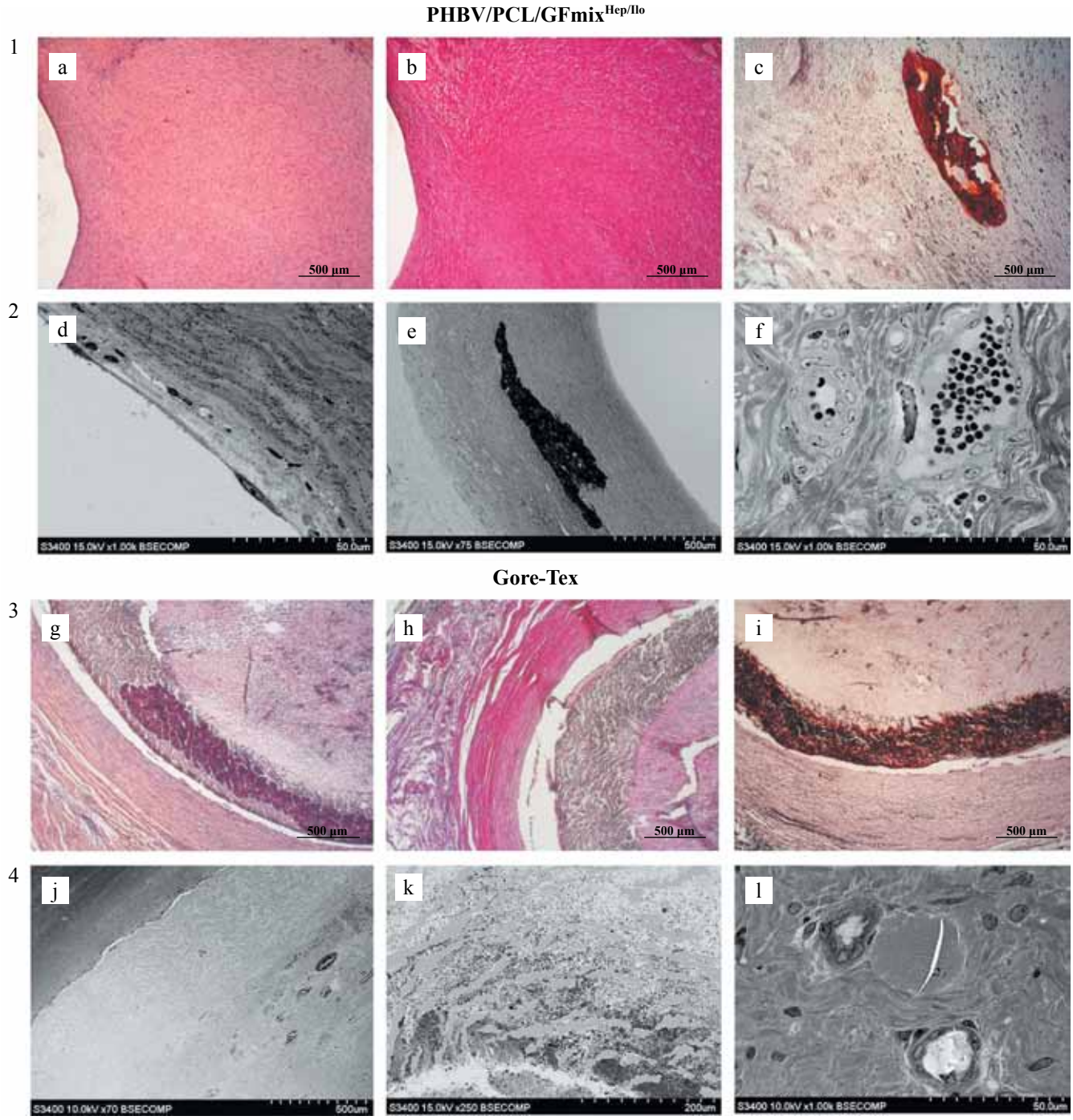

Fig. 3. Results of morphological study of explanted PHBV/PCL/GFmix$^{Hep/Ilo}$ vascular grafts 18 months after implantation: 1, histological study (a, H&E stain; b, Van Gieson's stain; c, alizarin red S stain), 50× magnification; 2, scanning electron microscopy (d, endothelium on the inner surface of the graft, 1000× magnification; e, transverse section of the explanted graft wall with a calcification area, 75× magnification; f, vasa vasorum, smooth muscle fibers in the middle layer of the graft, 1000× magnification). Results of morphological examination of explanted Gore-Tex® vascular grafts 6 months after implantation: 3, histological examination (g, H&E stain; h, Van Gieson's stain; i, alizarin red S stain), 50× magnification; 4, scanning electron microscopy (j, transverse section, 70× magnification; k, calcium in the graft wall thickness, 250× magnification; l, newly formed vessels in the outer sheath tissue, 1000× magnification)

no endothelial layer, neointima and media were found; no collagen type III was revealed, and only slight deposition of collagen type IV was found in the marginal zone on the inner lumen side (Fig. 4). Formation of connective tissue capsule with neorevascularization signs was detected on the outer surface of the explanted graft (Fig. 4).

Results of examination of the elemental composition of explanted vascular graft samples

A study of the elemental composition of solid calcium deposits showed their internal homogeneity in terms of their calcium and phosphorus content. The median value of the calcium to phosphorus ratio for various sites (n = 6) was 2.01, with a minimum of 1.96 and maximum of 2.05. In the calcium-containing areas, consisting predominantly of calcined fibers, the Ca/P ratio in the various fibers ranged from 1.2 to 2.32. It is likely that such differences in calcium content are due to the different calcification stages for specific fibers. In addition to biologically significant elements, about 2% fluorine was detected in the composition of prosthetic fibers, which indirectly indicates that the fibers themselves were intact at the initial calcification stages. In the areas with solid

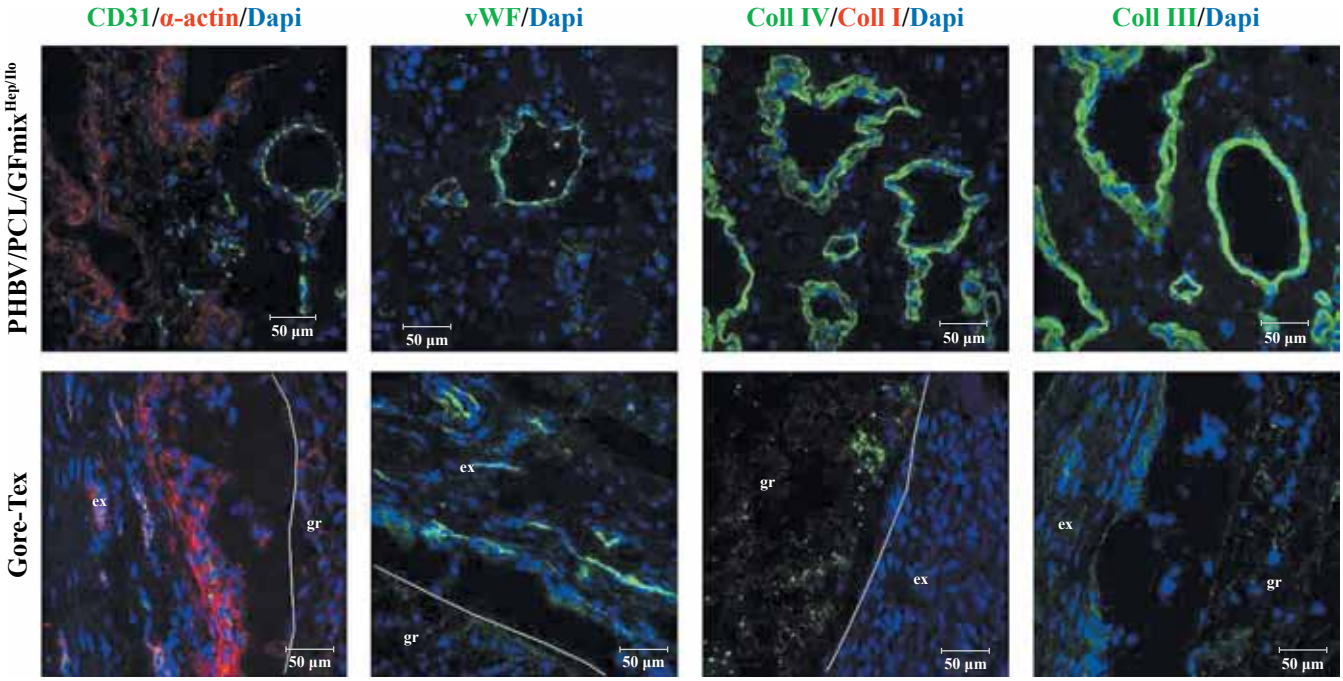

Fig. 4. Confocal microscopy of explanted vascular grafts PHBV/PCL/GFmix$^{Hep/Ilo}$ and Gore-Tex® staining with specific fluorescent anti-CD31 antibodies (mature endothelial cells), vWF (von Willebrand factor), α-actin (smooth muscle cell marker), collagen type I, collagen type III, collagen type IV, DAPI (fluorescent nuclear dye), 200× magnification

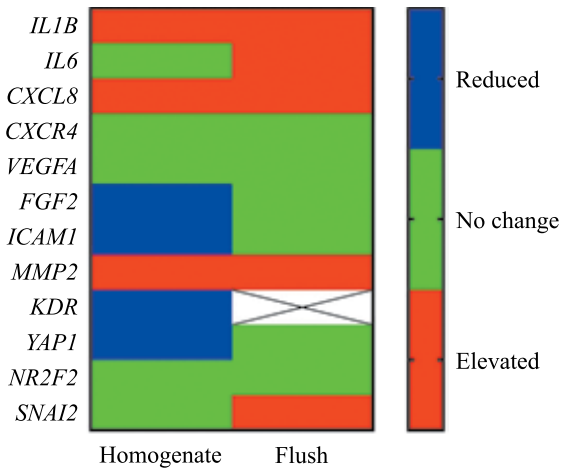

Fig. 5. Transcriptional profile of in situ regenerated PHBV/PCL/GFmix$^{Hep/Ilo}$ vascular grafts and intact contralateral carotid arteries 18 months after implantation

calcification inside the deposit, no fluoride was detected. This is probably due to the masking effect of the deposit itself, which reduces the accessibility of the probing electron beam inside the structure under study, rather than due to chemical destruction of the fibers.

Results of gene expression profile evaluation

The endothelial and wall transcription profiles of the regenerated artery were compared with those in the contralateral carotid arteries. Reverse transcription-quantitative polymerase chain reaction revealed an abundance of transcripts associated with inflammation (IL1B, IL6, and CXCL8), ECM remodeling (MMP2), and EndMT (SNAI2) in both RNA fractions obtained from the regenerated artery (Fig. 5). The endothelial lysate was enriched in inflammatory transcripts (IL1B, IL6, and ICAM1) and signs of endothelial reprogramming

(venous transcript NR2F2, and EndMT marker SNAI2) (Fig. 5). These observations suggest that the molecular landscape of the vascular tissue formed in place of the biodegradable vascular graft may differ from the corresponding blood vessels even during arterial regeneration in the long term (18 months after implantation).

CONCLUSION

The study on modification of vascular grafts made of PHBV/PCL polymer mixture using growth factors, as well as formation of a Hep + Ilo drug coating on the inner surface, attached through a PVP hydrogel coating by complexation method, showed successful creation of a highly porous and functionally active biodegradable vascular graft. It was on the basis of this graft that a newly formed vascular tissue similar in structure to the native carotid artery of a sheep can form over time. Also, the attachment of drug-containing hydrogel coating to the graft surface allowed to temporarily smooth the relief of the internal surface of the graft and enhance its anti-thrombogenic potential due to slow release of heparin and iloprost after implantation into the vascular bed. However, the presence of aneurysmal dilatation suggests that the newly formed tissue was incapable of resisting cyclic loads of blood flow. Therefore, despite the high biocompatibility obtained and the formation of newly-formed vascular tissue without initiation of inflammation and calcification processes, the outer frame of the developed design requires additional strengthening.

The research was done as part of a comprehensive scientific and technical program of a full innovation cycle "Development and introduction of a complex of technologies in the field of exploration and production of solid minerals, maintenance of industrial safety, bioremediation, creation of products of deep processing from coal raw materials, while consistently reducing the environmental impact and risks for the life of the population" (adopted by Order #1144r of the Government of the Russian Federation on May 11, 2022).

The authors declare no conflict of interest.

REFERENCES

1. *Benjamin EJ, Muntner P, Alonso A, Bittencourt MS, Callaway CW, Carson AP et al.* American Heart Association Council on Epidemiology and Prevention Statistics Committee and Stroke Statistics Subcommittee. Heart Disease and Stroke Statistics-2019 Update: A Report From the American Heart Association. *Circulation*. 2019; 139 (10): 56–528. doi: 10.1161/CIR.0000000000000659. PMID: 30700139.
2. *Virani SS, Alonso A, Benjamin EJ, Bittencourt MS, Callaway CW, Carson AP et al.* American Heart Association Council on Epidemiology and Prevention Statistics Committee and Stroke Statistics Subcommittee. Heart Disease and Stroke Statistics-2020 Update: A Report From the American Heart Association. *Circulation.* 2020; 141 (9): 139–596. doi: 10.1161/CIR.0000000000000757. PMID: 31992061.
3. *Virani SS, Alonso A, Aparicio HJ, Benjamin EJ, Bittencourt MS, Callaway CW et al*. American Heart Association Council on Epidemiology and Prevention Statistics Committee and Stroke Statistics Subcommittee. Heart Disease and Stroke Statistics-2021 Update: A Report From the American Heart Association. *Circulation*. 2021; 143 (8): 254–743. doi: 10.1161/CIR.0000000000000950. PMID: 33501848.
4. *Pashneh-Tala S, MacNeil S, Claeyssens F.* The Tissue-Engineered Vascular Graft-Past, Present, and Future. *Tissue Eng Part B Rev*. 2016; 22 (1): 68–100. doi: 10.1089/ten.teb.2015.0100. PMID: 26447530.
5. *Roth GA, Mensah GA, Johnson CO, Addolorato G, Ammirati E, Baddour LM et al.* Global Burden of Cardiovascular Diseases Writing Group. Global Burden of Cardiovascular Diseases and Risk Factors, 1990–2019: Update From the GBD 2019 Study. *J Am Coll Cardiol*. 2020; 76 (25): 2982–3021. doi: 10.1016/j.jacc.2020.11.010. PMID: 33309175.
6. *Taggart DP*. Current status of arterial grafts for coronary artery bypass grafting. *Ann Cardiothorac Surg.* 2013; 2 (4): 427–430. doi: 10.3978/j.issn.2225-319X.2013.07.21. PMID: 23977618.
7. *Elliott MB, Ginn B, Fukunishi T, Bedja D, Suresh A, Chen T et al.* Regenerative and durable small-diameter graft as an arterial conduit. *Proc Natl Acad Sci USA*. 2019; 116 (26): 12710–12719. doi: 10.1073/pnas.1905966116. PMID: 31182572.
8. *Kimicata M, Swamykumar P, Fisher JP*. Extracellular Matrix for Small-Diameter Vascular Grafts. *Tissue Eng Part A*. 2020; 26 (23–24): 1388–1401. doi: 10.1089/ten.TEA.2020.0201. PMID: 33231135.
9. *Matsushita H, Inoue T, Abdollahi S, Yeung E, Ong CS, Lui C et al*. Corrugated nanofiber tissue-engineered vascular graft to prevent kinking for arteriovenous shunts in an ovine model. *JVS Vasc Sci.* 2020; 1: 100–108. doi: 10.1016/j.jvssci.2020.03.003. PMID: 34617042.
10. *Matsuzaki Y, Ulziibayar A, Shoji T, Shinoka T*. Heparin-Eluting Tissue-Engineered Bioabsorbable Vascular Grafts. *Applied Sciences*. 2021; 11 (10): 4563. doi: 10.3390/app11104563.
11. *Aussel A, Thébaud NB, Bérard X, Brizzi V, Delmond S, Bareille R et al.* Chitosan-based hydrogels for developing a small-diameter vascular graft: *in vitro* and *in vivo* evaluation. *Biomed Mater*. 2017; 12 (6): 065003. doi: 10.1088/1748-605X/aa78d0. PMID: 28604360.
12. *Stowell CET, Wang Y.* Quickening: Translational design of resorbable synthetic vascular grafts. *Biomaterials*. 2018; 173: 71–86. doi: 10.1016/j.biomaterials. PMID: 29772461.
13. *Fernández-Colino A, Wolf F, Rütten S, Schmitz-Rode T, Rodríguez-Cabello JC, Jockenhoevel S, Mela P*. Small caliber compliant vascular grafts based on elastin-like recombinamers for *in situ* tissue engineering. *Front Bioeng Biotechnol*. 2019; 7: 340. doi: 10.3389/fbioe.2019.00340.
14. *Shoji T, Shinoka T*. Tissue engineered vascular grafts for pediatric cardiac surgery. *Transl Pediatr*. 2018; 7 (2): 188–195. doi: 10.21037/tp.2018.02.01. PMID: 29770300.

15. *Ren X, Feng Y, Guo J, Wang H, Li Q, Yang J et al*. Surface modification and endothelialization of biomaterials as potential scaffolds for vascular tissue engineering applications. *Chem Soc Rev*. 2015; 44 (15): 5680–5742. doi: 10.1039/c4cs00483c. PMID: 26023741.
16. *Wissing TB, Bonito V, Bouten CVC, Smits AIPM*. Biomaterial-driven *in situ* cardiovascular tissue engineering-a multi-disciplinary perspective. *NPJ Regen Med*. 2017; 2: 18. doi: 10.1038/s41536-017-0023-2. PMID: 29302354.
17. *Song HG, Rumma RT, Ozaki CK, Edelman ER, Chen CS*. Vascular Tissue Engineering: Progress, Challenges, and Clinical Promise. *Cell Stem Cell*. 2018; 22 (3): 340–354. doi: 10.1016/j.stem.2018.02.009. PMID: 29499152.
18. *Malik S, Sundarrajan S, Hussain T, Nazir A, Ramakrishna S*. Fabrication of Highly Oriented Cylindrical Polyacrylonitrile, Poly(lactide-co-glycolide), Polycaprolactone and Poly(vinyl acetate) Nanofibers for Vascular Graft Applications. *Polymers*. 2021; 13 (13): 2075. doi: 10.3390/polym13132075. PMID: 34202499.
19. *Drews JD, Pepper VK, Best CA, Szafron JM, Cheatham JP, Yates AR et al*. Spontaneous reversal of stenosis in tissue-engineered vascular grafts. *Sci Transl Med*. 2020; 12 (537): eaax6919. doi: 10.1126/scitranslmed.aax6919. PMID: 32238576.
20. *Cui H, Zhu W, Huang Y, Liu C, Yu ZX, Nowicki M et al*. *In vitro* and *in vivo* evaluation of 3D bioprinted small-diameter vasculature with smooth muscle and endothelium. *Biofabrication*. 2019; 12 (1): 015004. doi: 10.1088/1758-5090/ab402c. PMID: 31470437.
21. *Radke D, Jia W, Sharma D, Fena K, Wang G, Goldman J et al*. Tissue Engineering at the Blood-Contacting Surface: A Review of Challenges and Strategies in Vascular Graft Development. *Adv Healthc Mater*. 2018; 7 (15): e1701461. doi: 10.1002/adhm.201701461. PMID: 29732735.
22. *Matsuzaki Y, Miyamoto S, Miyachi H, Iwaki R, Shoji T, Blum K et al*. Improvement of a Novel Small-diameter Tissue-engineered Arterial Graft With Heparin Conjugation. *Ann Thorac Surg*. 2021; 111 (4): 1234–1241. doi: 10.1016/j.athoracsur.2020.06.112. PMID: 32946845.
23. *Matsuzaki Y, Iwaki R, Reinhardt JW, Chang YC, Miyamoto S, Kelly J et al*. The effect of pore diameter on neo-tissue formation in electrospun biodegradable tissue-engineered arterial grafts in a large animal model. *Acta Biomater*. 2020; 115: 176–184. doi: 10.1016/j.actbio.2020.08.011. PMID: 32822820.
24. *Fang S, Ellman DG, Andersen DC*. Review: Tissue Engineering of Small-Diameter Vascular Grafts and Their *In Vivo* Evaluation in Large Animals and Humans. *Cells*. 2021; 10 (3): 713. doi: 10.3390/cells10030713. PMID: 33807009.
25. *Jia W, Li M, Weng H, Gu G, Chen Z*. Design and comprehensive assessment of a biomimetic tri-layer tubular scaffold via biodegradable polymers for vascular tissue engineering applications. *Mater Sci Eng C Mater Biol Appl*. 2020; 110: 110717. doi: 10.1016/j.msec.2020.110717. PMID: 32204029.
26. *Norouzi SK, Shamloo A*. Bilayered heparinized vascular graft fabricated by combining electrospinning and freeze drying methods. *Mater Sci Eng C Mater Biol Appl*. 2019; 94: 1067–1076. doi: 10.1016/j.msec.2018.10.016. PMID: 30423687.
27. *Liu Yue, Jiang Ziyi, Li Jingjing, Meng Kai, Zhao Huijing*. Cell co-culture and *in vivo* biocompatibility of poly(L-lactic caprolactone)/silk fibroin small-diameter artificial blood vessels[J]. *Chinese Journal of Tissue Engineering Research*. 2022; 26 (22): 3505–3513. doi: 10.12307/2022.278.
28. *Yao W, Gu H, Hong T, Wang Y, Chen S, Mo X et al*. A bi-layered tubular scaffold for effective anti-coagulant in vascular tissue engineering. *Materials & Design*. 2020; 194: 108943. doi: 10.1016/j.matdes.2020.108943.
29. *Antonova LV, Sevostyanova VV, Mironov AV, Krivkina EO, Velikanova EA, Matveeva VG et al. In situ* vascular tissue remodeling using biodegradable tubular scaffolds with incorporated growth factors and chemoattractant molecules. *Complex Issues of Cardiovascular Diseases*. 2018; 7 (2): 25–36. doi: 10.17802/2306-1278-2018-7-2-25-36.
30. *Stowell CET, Li X, Matsunaga MH, Cockreham CB, Kelly KM, Cheetham J et al*. Resorbable vascular grafts show rapid cellularization and degradation in the ovine carotid. *J Tissue Eng Regen Med*. 2020; 14 (11): 1673–1684. doi: 10.1002/term.3128. PMID: 32893492.
31. *Zhu T, Gu H, Ma W, Zhang Q, Du J, Chen S et al*. A fabric reinforced small diameter tubular graft for rabbits' carotid artery defect. *Composites Part B: Engineering*. 2021; 225: 109274. doi: 10.1016/j.compositesb.2021.109274.
32. *Antonova LV, Sevostyanova VV, Rezvova MA, Krivkina EO, Kudryavtseva YuA, Barbarash OL, Barbarash LS*. Manufacturing technology of functionally active biodegradable vascular prostheses of small diameter with drug coating: Pat. 2702239. Applicant and patentee Federal State Budgetary Scientific Institution "Research Institute for Complex Problems of Cardiovascular Diseases" (NII KPSSZ) (RU); No. 2019119912; dec. 06/25/2019; publ. 07.10.2019, bull. No. 28 [In Russ].
33. *Abd El-Mohdy HL, Hegazy El-SA*. Preparation of Polyvinyl Pyrrolidone-Based Hydrogels by Radiation-Induced Crosslinking with Potential Application as Wound Dressing, *Journal of Macromolecular Science, Part A*. 2008; 45 (12): 995–1002. doi: 10.1080/10601320802454128.
34. *Godakanda, VU, Li H, Alquezar L, Zhao L, Zhu LM, de Silva R et al.* Tunable drug release from blend poly (vinyl pyrrolidone)-ethyl cellulose nanofibers. *International Journal of Pharmaceutics*. 2019; 562: 172–179. doi: 10.1016/j.ijpharm.2019.03.035.
35. *Antonova LV, Rezvova MA, Sevost'yanova VV, Tkachenko VO, Glushkova TV, Akent'eva TN, Kudryavtseva YuA, Barbarash LS.* Razrabotka tekhnologii formirovaniya atrombogennogo lekarstvennogo pokrytiya dlya biodegradiruemykh sosudistykh protezov. *Sovremennye tekhnologii v meditsine*. 2020; 12 (6): 6–14.
36. *Ahmed M, Hamilton G, Seifalian AM*. The performance of a small-calibre graft for vascular reconstructions in a senescent sheep model. *Biomaterials*. 2014; 35 (33): 9033–9040.
37. *Antonova LV, Mironov AV, Yuzhalin AE, Krivkina EO, Shabaev AR, Rezvova MA. et al.* Brief Report on an Implantation of Small-Caliber Biodegradable Vascular Grafts in a Carotid Artery of the Sheep. *Pharmaceuticals*. 2020; 13: 101. doi: 10.3390/ph13050101.

The article was submitted to the journal on 13.04.2022